HHS Public Access

Author manuscript

J Virol Methods. Author manuscript; available in PMC 2019 March 01.

Published in final edited form as:

J Virol Methods. 2018 March ; 253: 11–17. doi:10.1016/j.jviromet.2017.12.002.

Development of an *in vivo* infection model to study Mouse papillomavirus-1 (MmuPV1)

Aayushi Uberoi, **Satoshi Yoshida**, and **Paul F. Lambert***

McArdle Laboratory of Cancer Research, 1111 Highland Avenue, University of Wisconsin, Madison 53705, United States

Abstract

Preclinical model systems to study multiple features of the papillomavirus life cycle are extremely valuable tools to aid our understanding of Human Papillomavirus (HPV) biology, disease progression and treatments. Mouse papillomavirus (MmuPV1) is the first ever rodent papillomavirus that can infect the laboratory strain of mice and was discovered recently in 2011. This model is an attractive model to study papillomavirus pathogenesis due to the ubiquitous availability of lab mice and the fact that this mouse species is easily genetically modifiable. Several other groups, including ours, have reported that MmuPV1-induced papillomas are restricted to T-cell deficient immunosuppressed mice. In our lab we showed for the first time that MmuPV1 causes skin cancers in UVB-irradiated immunocompetent animals. In this report we describe in detail the MmuPV1-UV infection model that can be adapted to study MmuPV1 biology in immunocompetent animals.

Keywords

Mouse papillomavirus; Immunocompetent; Ultraviolet radiation; Preclinical model

1. Type of research

Papillomaviruses are species-specific, double-stranded DNA viruses that infect mucosal and cutaneous epithelia. Papillomaviruses have been identified throughout the animal kingdom and more than 180 types of human papillomaviruses (HPVs) have been identified (de Villiers et al., 2004). Mucosotropic HPVs are one of the most common sexually transmitted pathogens; of these, the high-risk subset causes over 5% of human cancers, including cervical cancer, other anogenital cancers, and a growing fraction of head and neck cancers [reviewed in McLaughlin-Drubin et al. (2012)]. A large subset of human papillomaviruses, belonging to the beta papillomavirus genera, infects cutaneous epithelia [reviewed in Meyers and Munger (2014), Jablonska et al. (1997, 1985)]. Cutaneous HPVs are found ubiquitously and frequently can be detected on asymptomatic skin. Low-risk cutaneous HPVs cause benign skin warts, which are the most common ailments treated by dermatologist (Tschandl et al., 2014), arising most frequently in children (Mammas et al., 2014; van Haalen et al., 2009) as well as immunocompromised patients, particularly organ transplant recipients

*Corresponding author. plambert@wisc.edu (P.F. Lambert).

(Antonsson et al., 2000; Astori et al., 1998; Gassenmaier et al., 1986; Connolly et al., 2014). Certain cutaneous HPVs are considered high-risk HPVs because they are causally associated with skin cancer [reviewed in Tommasino (2017), Howley and Pfister (2015), McLaughlin-Drubin (2015)]. Epidemiological studies have revealed a correlation between the level of exposure to ultraviolet radiation (UVR) and prevalence of cutaneous HPVs in healthy as well as immunosuppressed patients (Chen et al., 2008; Hampras et al., 2014; Reusser et al., 2015). Cutaneous HPVs are also more commonly found at anatomical sites exposed to sunlight, and a history of blistering sunburn is associated with prevalent and persistent cutaneous HPV infections (Chen et al., 2008; Hampras et al., 2014; Iannacone et al., 2010). A recent study in laboratory mice indicates UVR-enhanced susceptibility to papillomavirus-associated disease correlates with UV-induced immunosuppression (Uberoi et al.).

Because papillomaviruses (PVs) are species, it is challenging to study the pathogenesis caused by HPVs. Mice genetically engineered to express HPV genes have greatly advanced our understanding of HPV biology, particularly HPV-associated carcinogenesis [reviewed in Lambert (2016)]; however, they do not recapitulate the natural infectious disease caused by HPVs. Historically, bovine, canine and rabbit PVs have been used to study papillomavirus-associated disease [reviewed in Christensen et al. (2017), Bocaneti et al. (2016), Doorbar (2016), Gil da Costa et al. (2017)]. Over the years, a number of different rodent papillomaviruses were identified [reviewed in Christensen et al. (2017)] including the *Mastomys natalensis* papillomavirus that causes squamous cell carcinoma in the multimammate rat species (Helfrich et al., 2004; Muller and Gissmann, 1978; Salvermoser et al., 2016). However, no papillomavirus that infects laboratory mice had been identified, until recently. A papillomavirus (MmuPV1) that causes skin papillomas in *Mus musculus* was reported in 2011 (Joh et al., 2012; Meyers et al., 2017; Ingle et al., 2011) providing the first opportunity to study the life cycle and pathogenesis of papillomaviruses in the context of a genetically manipulatable, laboratory animal species (Bock et al., 2014; Walrath et al., 2010).

Multiple studies have shown that the ability of MmuPV1 to cause disease is largely restricted to immunodeficient strains of laboratory mice (Joh et al., 2012; Cladel et al., 2013; Handisurya et al., 2014; Sundberg et al., 2014; Wang et al., 2015). MmuPV1 causes warts in cutaneous epithelium as well as in mucosal epithelium lining the female reproductive tract and oral cavity and in some cases these lesions show signs of neoplastic progression (Cladel et al., 2013, 2015; Sundberg et al., 2014). Recently we made the novel observation that ultraviolet radiation (UVR), specifically the UVB spectra, caused wild type, immunocompetent strains of mice to become highly susceptible to MmuPV1-induced papillomas (Uberoi et al., 2016). We found that UVB induced systemic immunosuppression in these mice that correlated with susceptibility to MmuPV1-associated disease. Depending on the genetic background, 25–50% of sites infected with MmuPV1 in UVB-irradiated animals developed cutaneous papillomas and these papillomas had associated with them squamous cell carcinoma. This pathogenesis is similar to that of high-risk cutaneous HPVs. This similarity is born out at the molecular level; proteomic studies demonstrate that the MmuPV1 E6 protein has similar biochemical functions as the E6 protein encoded by the high-risk, cutaneous HPV, HPV8, which are quite distinct from the biochemical functions of

E6 proteins encoded by the high-risk, mucosotropic HPVs (Meyers et al., 2017). Thus, MmuPV1 is emerging as a valuable animal papillomavirus to study HPV-associated disease.

In this report we describe in detail the methods used to study MmuPV1-associated disease in immunocompetent strains of mice, as well as specific points to consider in designing experiments using MmuPV1.

2. Time required

- Infection of mice with MmuPV1 virus extract: 10–15 min per mouse
- UVB irradiation of infected animals: 5–10 min per cage
- Scoring of papillomas: 5–10 min per mouse
- It takes at least 6–8 weeks post-infection for papillomas to develop. In general, growth of papillomas was monitored over a period of 6 months.
- Harvesting papilloma tissue for histopathological analysis: 10 min.

3. Materials

3.1. Animals

FVB/NTac mice (6–8 weeks old) were obtained from Taconic and bred for this study. As positive control for determining whether virus is infections immunodeficient athymic BALB/c FoxN1$^{nu/nu}$ were obtained from Envigo. All animals were housed in autoclaved micro-isolator cages with individual water bottles. Athymic mice were housed under aseptic conditions. Infected mice were housed in a level 3 animal facility in a separate quarantine room dedicated to MmuPV1 experiments that was equipped with a biosafety level 2 (BSL2) cabinet in which all work with infected mice was carried out. Special precautions were taken to prevent spread of this virus between cages and throughout the vivarium. Animals were handled only by designated laboratory personnel (not the general animal facility staff) who, in addition to wearing standard personal protection equipment (PPE), changed gloves frequently among cages.

3.2. Special equipment

3.2.1. UVB irradiator—A custom-designed “Spectra” research irradiation unit (48″ unit, S. No. R2017-AXBX-0606, 110–120 V, 60 Hz) manufactured by Daavlin (Bryan, Ohio) was used for these studies [also described in Afaq et al. (2007), Calvo-Castro et al. (2013)]. The irradiator consists of an exposure unit (52″ × 27 ¼″ × 25″) mounted on fixed legs (Fig. 1a). The height of the irradiating surface to the lamps can be adjusted. Within the exposure unit there are six UVA lamps (F40T12BL/HO) and six UVB lamps (FS40T12HO-BB) lamps (Fig. 1b). These lamps are controlled using a Flex Control Integrating Dosimeters that automatically compensates for variations in energy output in order to deliver the desired UV dose with consistency and accuracy. Desired dosage is entered in milli-Joules per Centimeter Square for UVB (mJ/cm^2) and Joules per Centimeter Square for UVA (J/cm^2). The machine is periodically calibrated by the manufacturer using an International Light IL 1400, digital light meter, provided by the manufacturer such that UVB output is 2-4–2.9 mW/cm^2. This

output was measured using a UV meter provided by the manufacturer. To prevent exposure of user to UV, a UV blocking curtain is attached to the irradiator. The usable radiation area is approximately 40″ × 26″, allowing one to irradiate up to 3 mouse cages at a time.

3.2.2. Other equipment—Gaseous anesthesia (isoflurane) apparatus, Micrometer screw gauge (iGaging, California, #205630), hand-held magnifying glass, 27 gauge syringe needle, surgical equipment (forceps, scalpel, scissors), siliconized eppendorf tubes (Fisher Scientific, #02-681-320) and pipette tips (VWR, #83007-380), Tissue-tek cassette (VWR, #25608-774).

3.3. Reagents

3.3.1. MmuPV1 virions—Stocks of MmuPV1 virus were generated from MmuPV1-induced papillomas that arose in nude mice as described previously (Handisurya et al., 2014, 2012, 2013). Methods for isolation and quantification of virus particles from papillomas are available at protocols.io (Uberoi and Lambert, 2017). Protocols.io is an open access platform where detailed lab protocols can be uploaded and accessed using the provided DOI access information (Teytelman et al., 2016). We quantify the amount of virus particles in any given stock so that we can infect with a known amount of virus in each experiment. This is critical because we have found that the incidence of papillomatosis is dependent upon the dose of virus used (Uberoi et al., 2016). We use the standard of measuring the amount of encapsidated viral genomic DNA to determine the concentration of “viral genome equivalents” (VGE) in any given stock of virus. The original source of the MmuPV1 genome was generated by rolling circle amplification of DNA extracted from warts that arose in the original colony of mice in which the virus was identified (Ingle et al., 2011). This DNA stock was generously provided by Dr. Aravind Ingle (ACTREC, India). The viral genome was cloned into the Xba1 sites of pUC19 (Joh et al., 2011; Ingle et al., 2011) and quasivirions were generated as described previously (Handisurya et al., 2013; Pyeon et al., 2005) 2in which MmuPV1 genome, released from the bacterial plasmid vector by cleavage with Xba1 followed by recircularization by ligation under dilute conditions, was packaged into virions in 293FT cells (Invitrogen, #R70007) co-transfected with pMusSHELL, a mammalian expression plasmid carrying codon-optimized versions of the MmuPV1 major (L1) and minor (L2) capsid genes, generously provided by Dr. Chris Buck (NIH, Bethesda, MD) (Handisurya et al., 2012). Methods for generation of quasivirions are described in detail on Dr. Chris Buck’s (National Institute of Health, Bethesda) lab website: https://home.ccr.cancer.gov/LCO/production.asp. To establish a source for virus extract in labs, MmuPV1 infection model can be established infecting nude mice using MmuPV1 quasivirions or naked DNA as described previously (Ingle et al., 2011; Cladel et al., 2013; Sundberg et al., 2014; Handisurya et al., 2013).

4. Detailed procedure

4.1. Infection of mice with MmuPV1 virus extract

i. Carry out all procedures in a dedicated BSL2 hood. Clean hood surface with 5% dilute bleach, followed by distilled water, followed by 70% ethanol to decontaminate surfaces having possible papillomaviruses.

ii. Induce general anesthesia using 5% isoflurane in 100% oxygen (flow rate 2 l/min) and maintain anesthesia using 1–3% isoflurane.

iii. Ensure that the animal is under anesthesia throughout the procedure.

iv. Pre-scarify the inner surface of the mouse outer ear (pinna) first by gently scraping the epithelia using a sterile razor blade by scraping lightly 4–5 times over an area approximately 2 × 2 mm^2. Try remaining within the center of the ear so that you are not at the edge of the pinna.

v. Use a sterile 27-gauge syringe needle to go over the pre-scarified surface at least 10–15 times to create a “brush-burn” like lesion. This should be a superficial wound such that there is enough wounding for the virus to reach the basal layer (pink-red in color) but taking care to not cause profuse bleeding. The ear is thin so take care to not pierce through it. To prevent this from occurring you may need to provide support to the pinna using a curved surface such as a round bottom falcon tube or by orienting the animal so that the ear is resting on a flat surface. Sufficient scarring is achieved when you can see a lesion that represents a partial thickness open wound. Since the ear capillaries very fine it is possible to cause some bleeding in which case pressing the wound site and wiping it with gauze should stop the wounding.

vi. Administer the virus solution (less than 3 μl) at site of scarification using a siliconized pipette tip. The animal is kept under anesthesia for at least 5 more minutes so that the virus solution dries up at which point the animal is returned to the cage. To prevent post-anesthesia hypothermia the animal may be placed over a heating pad until recovery.

4.2. UVB irradiation of infected animals

vii. UVB irradiation of animals is most commonly performed 24 h post infection. To transport the animals transfer them to clean microisolator cages and reserve the original cages in the animal housing room.

viii. Wipe the irradiation surface with 70% ethanol and sterilize the area by running UVB light source by setting the UVB dose to desired dosage in mJ/cm^2 (we use 300 mJ/cm^2–500 mJ/cm^2 for FVB mice) according to machine operating instructions.

ix. Remove the plastic lid of the microisolator cage (leaving the cage wire on) and place cage under the UVB lamps in the UV exposure unit (Fig. 1). Draw out UV blocking curtain to shield user from UV light. At one time up to 3 cages can be placed under the lamps in this instrument

x. Turn on the UVB light source and wait till programmed dose is reached. The UV lamps will turn off immediately and you can remove the cages from the exposure unit.

xi. Wipe the irradiation surface with 70% ethanol and run the UV lamps to sterilize the work area.

xii. The animals should be returned to their original cages and the cages used for transporting the animals should be sent for washing.

4.3. Scoring of papillomas

xiii. Animals should be monitored for PV-associated disease at least once a week until reaching the end-point of the study.

xiv. To aid scoring process animals should be anesthetized using isoflurane. Using hand held magnifying glass and forceps to tease apart the ear skin is helpful in the scoring process.

xv. Start measuring size of papillomas 1–2 weeks after onset of papillomas by recording length, width and thickness of the papilloma by means of a micrometer screw gauge.

xvi. To measure the length and width of the papilloma place micrometer measuring faces along Y-axis and X-axis as indicated in Fig. 2.

xvii. The thickness of the papilloma is obtained by subtracting the measurement of the papilloma-free edge of the pinna from the measurement of the thickest part of the papilloma.

xviii. The size of the papilloma should be reported by calculating the geometric mean diameter (GMD; cubic root of the product of length × width × thickness)

xix. Papilloma incidence can be determined with accuracy 6–8 weeks post-infection or when papilloma GMD is at least 2 mm.

xx. Papilloma incidence (expressed as a percentage) is the: (# sites with overt papillomas/# of sites infected) × 100.

4.4. Harvesting papilloma tissue for histopathological analysis

xxi. Euthanize the animal from which tissue has to be harvested by CO_2 exposure as per IACUC guidelines.

xxii. Harvest papilloma by cutting pinna off at base using surgical scissors. It may be necessary to remove hair so that hair is not embedded in the paraffin block because hair can damage the microtome blade, and lead to tearing of thin sections.

xxiii. Using a scalpel trim off the excess non-papillomatosis tissue. Flatten tissue on a piece of whattmann paper cut to fit in the tissue cassette. Place a thin tissue sponge over the tissue and place this whattman paper-tissue-sponge sandwich in a tissue cassette.

xxiv. Fix tissue by placing cassette in a beaker containing 4% paraformaldehyde (PFA) in PBS (15–20 times volume of cassette, approximately 200mls for 4–5 cassettes) for 10–12 h at 4 °C.

xxv. Discard the PFA solution and rinse cassettes with 70% ethanol 2–3 times to remove residual PFA. Fill the container with 70% ethanol (15–20 times the volume of cassette) and store at 4 °C until ready to process and embed.

xxvi. After dehydrating sample as per standard processing protocol, embed the tissue on edge in a paraffin block such that sections are made of the cross section of the pinna.

xxvii. Tissue is sectioned at 5 μm and at least 25 serial sections are taken. H&E staining is performed on every 5th section. MmuPV1 DNA or viral capsid proteins (L1) can be detected by DNA *in situ* hybridization and immunohistochemistry/ immunofluorescence respectively, to confirm viral infection. Our detailed L1-Krt14 dual staining immunofluorescence protocol is described elsewhere (Uberoi et al., 2017). The protocol for DNA FISH can be modified for MmuPV1 as described previously (Makielski et al., 2016). Isolation of infectious MmuPV1 virions can be further performed to verify presence of MmuPV1 or test virus infectivity by serially passaging virus to other mice (Uberoi and Lambert, 2017).

5. Results

Morphological features of ears observed in mice post-infection and UVB irradiation are described in Table 1 and illustrated in Fig. 3. Under standard conditions in which we infect scarified pinna of FVB/NTac mice with 10^8 VGEs of MmuPV1 and irradiate with 300 mJ/cm^2, papillomas arise at approximately 50% of infected sites 6–8 weeks post-infection and continue to arise up to 3–4 months post-infection. The 3–4 month time-frame is the peak incidence of papillomatosis. These data have been described in depth previously (Uberoi et al., 2016). In animals where papillomas do not arise, skin returns to its normal appearance within 2–3 weeks post-infection. The developed papillomas can have either of the following characteristics:

- **i.** Progress to squamous cell carcinoma
- **ii.** Continue to grow in size
- **iii.** Decrease in size, i.e. regress
- **iv.** Completely regress

It is critical to monitor papillomas weekly after the 3 month time-point as some papillomas can completely regress very quickly.

6. Troubleshooting

6.1. Considerations to keep in mind while performing MmuPV1-infection studies

- **i.** Preventing contamination with MmuPV1 in the animal facility

  MmuPV1 naturally infects laboratory strains of mice. We recommend personnel to diligently follow necessary precautions in handling animals infected with the virus to prevent spread to uninfected mice housed in the same room and mice located elsewhere in the vivarium. Several publications from Dr. Craig Meyers group describe reagents that are effective in decontaminating area and equipment in contact with papillomaviruses. We suggest that users familiarize themselves with these publications (Meyers et al., 2014; Ryndock et al., 2016). We

recommend decontaminating areas and tools with 5% bleach followed by rinsing with water followed by wiping with 70% ethanol.

ii. Lack of papillomas in mice 16 weeks post-infection

a. In our experience, the incidence of MmuPV1-induced papillomas arising in immunocompetent strains of mice is dependent upon 4 main variables: the dose of virus, the strain of mouse, the method of scarification, and the UVB dose. Therefore, we recommend using a significantly large sample size. In our statistical determination via power analysis we have found this number to be greater than 12 sites of infection.

b. In this thesis, we described incidence of 50% when infecting the pinna of UVB-treated FVB/NTac mice with 10^8 VGE of MmuPV1. Papillomas can also arise in C57/BL6 and BALB/c mice with higher doses of UVB (Uberoi et al., 2016). While UVB causes immunosuppression in both FVB and C57/BL6, the FVB strain is classically used for skin cancer studies (Hennings et al., 1993); and, therefore, is the strain we have preferred to use in studying neoplastic disease induced by MmuPV1. If using a different genetic background we recommend titrating the dose of UVB to achieve the desired incidence. For example, we have found UVB doses between 600 and 1000 mJ/cm^2 to induce MmuPV1-associated papillomatosis in 30–50% of sites on the pinna of C57/BL6 mice infected with 10^8 MmuPV1 VGE per site (Uberoi et al., 2016).

c. We do not recommend freeze thawing stocks of virus, especially when working with crude viral extracts as this reduces the infectivity of the virus stock. Also see point (iii) for virus dose considerations.

d. It is important that the manufacturer calibrate the UVB irradiator equipment periodically so that the correct dose of UVB is delivered to the animals. It may be recommended to anesthetize or singly house animals during UVB irradiation so that the animals receive similar exposure of UVB. If using a different source of UVB, it may be necessary to optimize the UVB dose in experimenters' hand.

iii. Amount of virus to use

We have consistently seen papillomatosis arising on the ears of UVB-treated mice on different genetic backgrounds infected with 10^8 MmuPV1 VGE per site. In FVB/NTac mice, a minimum of 10^7 MmuPV1 VGE is required to see papilloma induction in this model. In contrast, in immunodeficient nude mice we have seen papillomatosis arise with 10^6 MmuPV1 VGE (Uberoi et al., 2016). The reasons for this observation remain to be investigated but we can conclude that a higher threshold of virus is required to see papilloma induction in immunocompetent mice treated with UVB. If using a virus amount less than 10^7 VGE, it is possible that one may not see papillomas develop up to 6-months post-

infection. It has been reported that some immunocompetent strains of mice not exposed to UVB are susceptible to MmuPV1 infection if using greater that 10^{11} MmuPV1 VGE, however these papillomas completely regressed within a month of appearing (Handisurya et al., 2013). In our hands 10^{8} VGE dose virus particles does not cause papillomas in non-UVB-irradiated, immunocompetent strains of mice.

iv. Control groups

For every experiment we recommend having the following control groups:

1. Athymic group of mice (n = 3) to test whether the virus stock is infectious
2. Non UVB-irradiated immunecompetent mice (n > 4) as a negative control
3. UVB-irradiated mock-infected mice (n > 4) as a negative control

v. Scoring papillomas

It is recommended to monitor animals daily for at least one week post-infection. If animals do not look healthy or appear in any discomfort, we recommend treating the animals with analgesics by injection or in drinking water. Following this period, we recommend scoring of papillomas weekly. It is possible to mistake swelling, edema and scabs for papillomas in the initial weeks following infection. For this reason, we recommend observing the animal carefully under anesthesia and using a hand-held magnifying glass if necessary. It may be beneficial to wait for a few days, as the papillomas are usually harder to diagnose at onset earlier than 3 months post-infection at which time they continue to grow in size. Re-evaluation of the same site can provide further confidence that there is a progressive increase in size of the emerging wart. If measuring papilloma size, we strongly recommend that one person perform all size measurements to ensure consistency. For each measurement, we take three independent reads and then use the average. In addition to scoring size of papillomas over time, photo-documentation of each site can provide a useful temporal record of disease. If tracking animals longitudinally, we recommend identifying animals by tattooing the tail or notching the edge of the ear. We do not recommend ear tagging for these studies as ear tagging has itself been reported to promote inflammation and skin cancer in mice (Baron et al., 2005; Kitagaki and Hirota, 2007). Papillomatosis should be confirmed via histopathology by consulting a pathologist.

vi. Timing for UVB irradiation

Most studies described in this thesis involve UVB irradiation 24 h post-infection. However, we have seen no difference in papilloma onset at the following time points: (i) 24-h prior to infection (Uberoi et al., 2016), (ii) 5 days post-infection, or (iii) 5 days prior to infection.

Variability in wounding and delivering of virus particles at infection site

Perhaps the greatest variability that can arise in this infection model is performing wounding of the infection site. This has been reported to be an important factor during characterization of the infection model for cottontail rabbit papillomavirus (CRPV) as well (Cladel et al., 2010). When infecting tail sites in immunosuppressed mice, other groups have reported wounding animals and then injecting virus particles 3 days post-wounding under the scab using a needle (Cladel et al., 2013, 2008). Our preferred site of infection is the ear, in which case it is difficult to inject under the scab due to ear thickness and curvature of the ear. Therefore we pipetted the virus solution directly onto the wounded site immediately after scarification. To adopt this approach, it is essential to have the virus in a minimal volume (e.g. 1–3 μl) so that the virus solution dries quickly post-application before returning the animal to its cage. Another way to deliver the virus is via intraderm injections. In our hands we found that intraderm injection at ear following scarification caused papillomas in athymic nude mice but we have not tested this approach in the context of the UVB-infection model. It is worth noting that, in the context of CRPV-based infection studies, intradermal injection was found to be inconsistent in causing papillomas. The authors noted that this might be due to the depth of delivery by intraderm injection, which could result in the virus only being delivered to the dermis (Reuter et al., 2001).

As we have reported in the detailed protocol (Section 4.1), the goal of the wounding is to create a “brush-burn” like lesion while taking care to not cause profuse bleeding. Since the mouse pinna is delicate, it is important to take care to not pierce or cut the ear while causing the wound. It is worth noting that the depth of wounding may differ from one person to the other, so we strongly recommend that one person perform all the wounding in a single experiment to reduce the concern of intra-experimental variation. We found it easiest to wound using a 27-gauge syringe needle but it might be useful to test other methods of wounding as described by other investigators (Handisurya et al., 2012). For all of these reasons, we recommend optimizing ear infection technique using nude mice first, and using nude mice as a positive control in parallel for each experiment.

7. Quick procedure

i. Anesthetize mice and pre-scarify inner ear using a 27-gauge needle to create a superficial wound

ii. Administer virus solution at the site of scarification and allow the solution to dry by keeping animal under anesthesia for at least 5 more minutes.

iii. UVB-irradiate animals 24 h later.

iv. Score papillomas at least once a week until the end-point of the study.

v. At the end point of the study harvest papilloma for histopathological analysis by paraformaldehyde fixation.

Acknowledgments

We thank Amy Liem(University of Wisconsin-Madison) for assisting in animal experiments; members of RARC, in particular – Terry Fritter, Satya Kishore (Animal care staff), Jim Taubel (facility incharge), Rachel C. Glab (RARC Vet) for providing animal care and assistance; Dr. Deeba Syed (Dr. Laboratory of Dr. Hasan Mukhtar, Department of Dermatology, University of Wisconsin-Madison) for guidance on using the UV irradiator; UWCC histology facility for embedding and sectioning tissue; Dr. Chris Buck (National Cancer Institute, Bethesda, MD) for providing us with antibody against L1 and plasmids. This work was supported by grants from the National Institutes of Health (CA022443, CA210807).

References

Afaq F, Syed DN, Malik A, Hadi N, Sarfaraz S, Kweon MH, Khan N, Zaid MA, Mukhtar H. Delphinidin, an anthocyanidin in pigmented fruits and vegetables, protects human HaCaT keratinocytes and mouse skin against UVB-mediated oxidative stress and apoptosis. J Invest Dermatol. 2007; 127:222–232. [PubMed: 16902416]

Antonsson A, Forslund O, Ekberg H, Sterner G, Hansson BG. The ubiquity and impressive genomic diversity of human skin papillomaviruses suggest a commensalic nature of these viruses. J Virol. 2000; 74:11636–11641. [PubMed: 11090162]

Astori G, Lavergne D, Benton C, Hockmayr B, Egawa K, Garbe C, de Villiers EM. Human papillomaviruses are commonly found in normal skin of immunocompetent hosts. J Invest Dermatol. 1998; 110:752–755. [PubMed: 9579540]

Baron BW, Langan G, Huo D, Baron JM, Montag A. Squamous cell carcinomas of the skin at ear tag sites in aged FVB/N mice. Comp Med. 2005; 55:231–235. [PubMed: 16089170]

Bocaneti F, Altamura G, Corteggio A, Velescu E, Roperto F, Borzacchiello G. Bovine papillomavirus: new insights into an old disease. Transbound Emerg Dis. 2016; 63:14–23.

Bock BC, Stein U, Schmitt CA, Augustin HG. Mouse models of human cancer. Cancer Res. 2014; 74:4671–4675. [PubMed: 25136075]

Calvo-Castro L, Syed DN, Chamcheu JC, Vilela FM, Perez AM, Vaillant F, Rojas M, Mukhtar H. Protective effect of tropical highland blackberry juice (Rubus adenotrichos Schltdl) against UVB-mediated damage in human epidermal keratinocytes and in a reconstituted skin equivalent model. Photochem Photobiol. 2013; 89:1199–1207. [PubMed: 23711186]

Chen AC, McMillan NA, Antonsson A. Human papillomavirus type spectrum in normal skin of individuals with or without a history of frequent sun exposure. J Gen Virol. 2008; 89:2891–2897. [PubMed: 18931088]

Christensen ND, Budgeon LR, Cladel NM, Hu J. Recent advances in preclinical model systems for papillomaviruses. Virus Res. 2017; 231:108–118. [PubMed: 27956145]

Cladel NM, Hu J, Balogh K, Mejia A, Christensen ND. Wounding prior to challenge substantially improves infectivity of cottontail rabbit papillomavirus and allows for standardization of infection. J Virol Methods. 2008; 148:34–39. [PubMed: 18061687]

Cladel NM, Hu J, Balogh KK, Christensen ND. Differences in methodology, but not differences in viral strain, account for variable experimental outcomes in laboratories utilizing the cottontail rabbit papillomavirus model. J Virol Methods. 2010; 165:36–41. [PubMed: 20036285]

Cladel NM, Budgeon LR, Cooper TK, Balogh KK, Hu J, Christensen ND. Secondary infections, expanded tissue tropism, and evidence for malignant potential in immunocompromised mice infected with Mus musculus papillomavirus 1 DNA and virus. J Virol. 2013; 87:9391–9395. [PubMed: 23785210]

Cladel NM, Budgeon LR, Balogh KK, Cooper TK, Hu J, Christensen ND. A novel pre-clinical murine model to study the life cycle and progression of cervical and anal papillomavirus infections. PLoS One. 2015; 10:e0120128. [PubMed: 25803616]

Connolly K, Manders P, Earls P, Epstein RJ. Papillomavirus-associated squamous skin cancers following transplant immunosuppression: one Notch closer to control. Cancer Treat Rev. 2014; 40:205–214. [PubMed: 24051018]

de Villiers EM, Fauquet C, Broker TR, Bernard HU, zur Hausen H. Classification of papillomaviruses. Virology. 2004; 324:17–27. [PubMed: 15183049]

Doorbar J. Model systems of human papillomavirus-associated disease. J Pathol. 2016; 238:166–179. [PubMed: 26456009]

Gassenmaier A, Fuchs P, Schell H, Pfister H. Papillomavirus DNA in warts of immunosuppressed renal allograft recipients. Arch Dermatol Res. 1986; 278:219–223. [PubMed: 3015050]

Gil da Costa RM, Peleteiro MC, Pires MA, DiMaio D. An update on canine, feline and bovine papillomaviruses. Transbound Emerg Dis. 2017 Oct; 64(5):1371–1379. http://dx.doi.org/10.1111/tbed.12555. [PubMed: 27615361]

Hampras SS, Giuliano AR, Lin HY, Fisher KJ, Abrahamsen ME, Sirak BA, Iannacone MR, Gheit T, Tommasino M, Rollison DE. Natural history of cutaneous human papillomavirus (HPV) infection in men: the HIM study. PLoS One. 2014; 9:e104843. [PubMed: 25198694]

Handisurya A, Day PM, Thompson CD, Buck CB, Kwak K, Roden RB, Lowy DR, Schiller JT. Murine skin and vaginal mucosa are similarly susceptible to infection by pseudovirions of different papillomavirus classifications and species. Virology. 2012; 433:385–394. [PubMed: 22985477]

Handisurya A, Day PM, Thompson CD, Buck CB, Pang YY, Lowy DR, Schiller JT. Characterization of Mus musculus papillomavirus 1 infection in situ reveals an unusual pattern of late gene expression and capsid protein localization. J Virol. 2013; 87:13214–13225. [PubMed: 24067981]

Handisurya A, Day PM, Thompson CD, Bonelli M, Lowy DR, Schiller JT. Strain-specific properties and T cells regulate the susceptibility to papilloma induction by Mus musculus papillomavirus 1. PLoS Pathog. 2014; 10:e1004314. [PubMed: 25121947]

Helfrich I, Chen M, Schmidt R, Furstenberger G, Kopp-Schneider A, Trick D, Grone HJ, Zur Hausen H, Rosl F. Increased incidence of squamous cell carcinomas in Mastomys natalensis papillomavirus E6 transgenic mice during two-stage skin carcinogenesis. J Virol. 2004; 78:4797–4805. [PubMed: 15078961]

Hennings H, Glick AB, Lowry DT, Krsmanovic LS, Sly LM, Yuspa SH. FVB/N mice: an inbred strain sensitive to the chemical induction of squamous cell carcinomas in the skin. Carcinogenesis. 1993; 14:2353–2358. [PubMed: 8242866]

Howley PM, Pfister HJ. Beta genus papillomaviruses and skin cancer. Virology. 2015:479–480. 290–296.

Iannacone MR, Michael KM, Giuliano AR, Waterboer T, Pawlita M, Rollison DE. Risk factors for cutaneous human papillomavirus seroreactivity among patients undergoing skin cancer screening in Florida. J Infect Dis. 2010; 201:760–769. [PubMed: 20105078]

Ingle A, Ghim S, Joh J, Chepkoech I, Bennett Jenson A, Sundberg JP. Novel laboratory mouse papillomavirus (MusPV) infection. Vet Pathol. 2011; 48:500–505. [PubMed: 20685915]

Jablonska S, Orth G, Obalek S, Croissant O. Cutaneous warts. Clinical, histologic, and virologic correlations. Clin Dermatol. 1985; 3:71–82. [PubMed: 2850861]

Jablonska S, Majewski S, Obalek S, Orth G. Cutaneous warts. Clin Dermatol. 1997; 15:309–319. [PubMed: 9255438]

Joh J, Jenson AB, King W, Proctor M, Ingle A, Sundberg JP, Ghim SJ. Genomic analysis of the first laboratory-mouse papillomavirus. J Gen Virol. 2011; 92:692–698. [PubMed: 21084500]

Joh J, Jenson AB, Proctor M, Ingle A, Silva KA, Potter CS, Sundberg JP, Ghim SJ. Molecular diagnosis of a laboratory mouse papillomavirus (MusPV). Exp Mol Pathol. 2012; 93:416–421. [PubMed: 22796029]

Kitagaki M, Hirota M. Auricular chondritis caused by metal ear tagging in C57BL/6 mice. Vet Pathol. 2007; 44:458–466. [PubMed: 17606507]

Lambert PF. Transgenic mouse models of tumor virus action. Annu Rev Virol. 2016; 3:473–489. [PubMed: 27741405]

Makielski KR, Lee D, Lorenz LD, Nawandar DM, Chiu YF, Kenney SC, Lambert PF. Human papillomavirus promotes Epstein-Barr virus maintenance and lytic reactivation in immortalized oral keratinocytes. Virology. 2016; 495:52–62. [PubMed: 27179345]

Mammas IN, Spandidos DA, Sourvinos G. Genomic diversity of human papillomaviruses (HPV) and clinical implications: an overview in adulthood and childhood. Infect Genet Evol. 2014; 21:220–226. [PubMed: 24291228]

McLaughlin-Drubin ME, Meyers J, Munger K. Cancer associated human papillomaviruses. Curr Opin Virol. 2012; 2:459–466. [PubMed: 22658985]

McLaughlin-Drubin ME. Human papillomaviruses and non-melanoma skin cancer. Semin Oncol. 2015; 42:284–290. [PubMed: 25843732]

Meyers JM, Munger K. The viral etiology of skin cancer. J Invest Dermatol. 2014; 134:E29–32. [PubMed: 25302471]

Meyers J, Ryndock E, Conway MJ, Meyers C, Robison R. Susceptibility of high-risk human papillomavirus type 16 to clinical disinfectants. J Antimicrob Chemother. 2014; 69:1546–1550. [PubMed: 24500190]

Meyers JM, Uberoi A, Grace M, Lambert PF, Munger K. Cutaneous HPV8 and MmuPV1 E6 proteins target the NOTCH and TGF-beta tumor suppressors to inhibit differentiation and sustain keratinocyte proliferation. PLoS Pathog. 2017; 13:e1006171. [PubMed: 28107544]

Muller H, Gissmann L. Mastomys natalensis papilloma virus (MnPV), the causative agent of epithelial proliferations: characterization of the virus particle. J Gen Virol. 1978; 41:315–323. [PubMed: 214519]

Pyeon D, Lambert PF, Ahlquist P. Production of infectious human papillomavirus independently of viral replication and epithelial cell differentiation. Proc Natl Acad Sci U S A. 2005; 102:9311–9316. [PubMed: 15958530]

Reusser NM, Downing C, Guidry J, Tyring SK. HPV carcinomas in immunocompromised patients. J Clin Med. 2015; 4:260–281. [PubMed: 26239127]

Reuter JD, Gomez D, Brandsma JL, Rose JK, Roberts A. Optimization of cottontail rabbit papilloma virus challenge technique. J Virol Methods. 2001; 98:127–134. [PubMed: 11576639]

Ryndock E, Robison R, Meyers C. Susceptibility of HPV16 and 18 to high level disinfectants indicated for semi-critical ultrasound probes. J Med Virol. 2016; 88:1076–1080. [PubMed: 26519866]

Salvermoser M, Chotewutmontri S, Braspenning-Wesch I, Hasche D, Rosl F, Vinzon SE. Transcriptome analysis of Mastomys natalensis papillomavirus in productive lesions after natural infection. J Gen Virol. 2016; 97:1658–1669. [PubMed: 27043420]

Sundberg JP, Stearns TM, Joh J, Proctor M, Ingle A, Silva KA, Dadras SS, Jenson AB, Ghim SJ. Immune status, strain background, and anatomic site of inoculation affect mouse papillomavirus (MmuPV1) induction of exophytic papillomas or endophytic trichoblastomas. PLoS One. 2014; 9:e113582. [PubMed: 25474466]

Teytelman L, Stoliartchouk A, Kindler L, Hurwitz BL. Protocolsio: virtual communities for protocol development and discussion. PLoS Biol. 2016; 14:e1002538. [PubMed: 27547938]

Tommasino M. The biology of beta human papillomaviruses. Virus Res. 2017; 231:128–138. [PubMed: 27856220]

Tschandl P, Rosendahl C, Kittler H. Cutaneous human papillomavirus infection: manifestations and diagnosis. Curr Probl Dermatol. 2014; 45:92–97. [PubMed: 24643180]

Uberoi, A., Lambert, PF. Isolation and quantification of MmuPV1 virions from papillomas. Protocolsio. 2017. http://dx.doi.org/10.17504/protocols.io.j8scrwe.1509473562

Uberoi A, Yoshida S, Frazer IH, Pitot HC, Lambert PF. Role of ultraviolet radiation in papillomavirus-induced disease. PLoS Pathog. 2016; 12:e1005664. [PubMed: 27244228]

Uberoi, A., Yoshida, S., Lambert, PF. MmuP L1- cytokeratin dual immunofluorescence using home-based tyramide signal amplification. Protocolsio. 2017. http://dx.doi.org/10.17504/protocols.io.i8cchsw

van Haalen FM, Bruggink SC, Gussekloo J, Assendelft WJ, Eekhof JA. Warts in primary schoolchildren: prevalence and relation with environmental factors. Br J Dermatol. 2009; 161:148–152. [PubMed: 19438464]

Walrath JC, Hawes JJ, Van Dyke T, Reilly KM. Genetically engineered mouse models in cancer research. Adv Cancer Res. 2010; 106:113–164. [PubMed: 20399958]

Wang JW, Jiang R, Peng S, Chang YN, Hung CF, Roden RB. Immunologic control of mus musculus papillomavirus type 1. PLoS Pathog. 2015; 11:e1005243. [PubMed: 26495972]

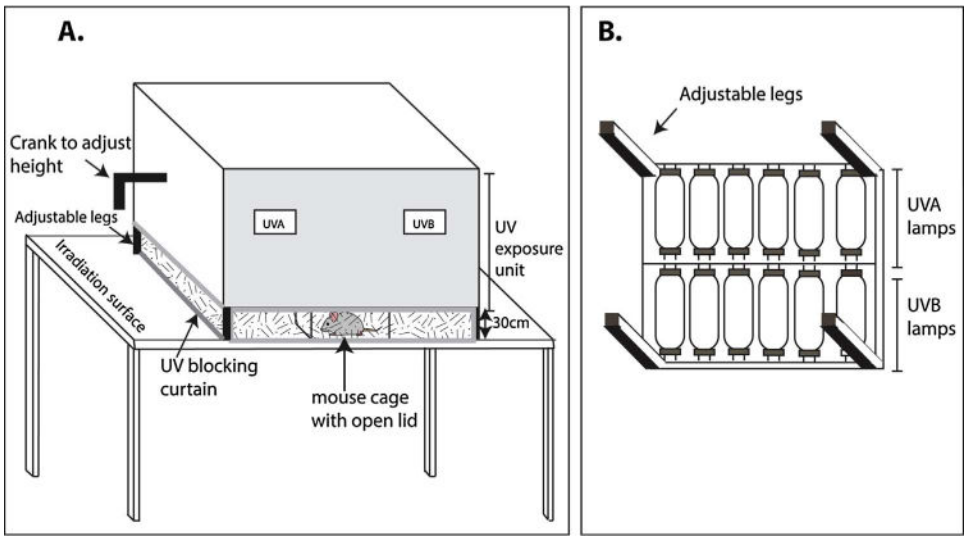

Fig. 1.
UV irradiator.

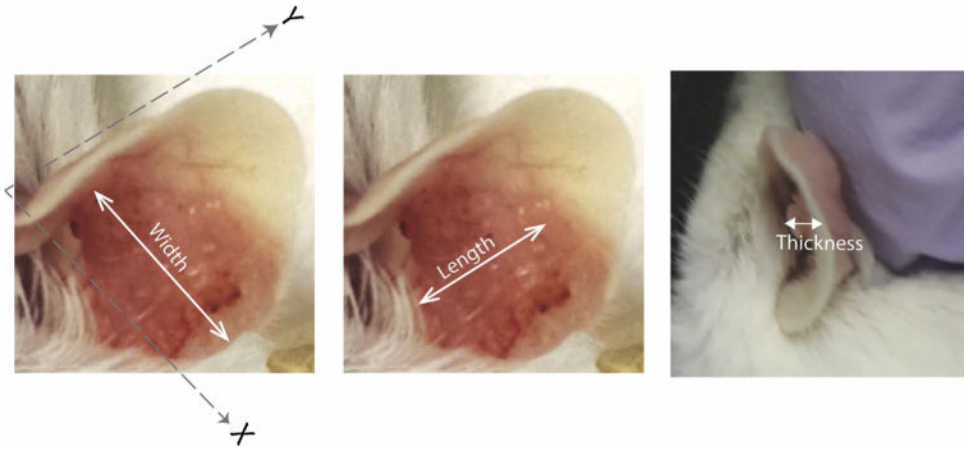

Fig. 2.
Size measurement.

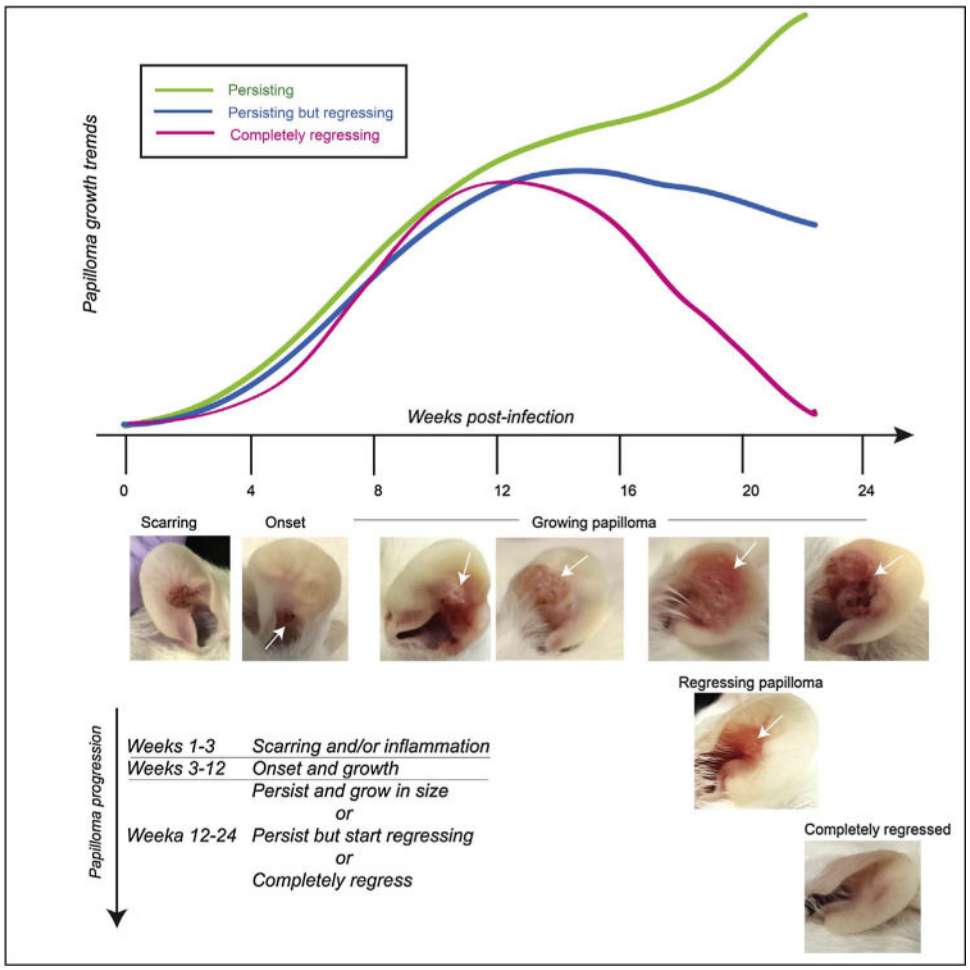

Fig. 3.
Growth profiles.

Table 1

Description of morphological features post infection (PI) with MmuPV1.

Time	Morphology	Description
Week 1	Wounding	• Partial thickness wound (4 mm^2) • Some wounds may have accompanying swelling • Some reddening of ears can be seen post UVB irradiation up to 48 h post treatment. • Several wounds start healing 3–4 days PI
Weeks 1–3	Scarring and/or edema	• Scabs are apparent 4–7 days PI • Some scars may be hypertrophic • In some cases swelling may be seen up to 2 weeks PI
Weeks 3–5	Skin healing without papilloma development (In a subset of mice)	• Scars flatten • Normal looking skin is restored
Weeks 3–12	Papilloma onset and growth (In another subset of mice)	• Clusters of white-brown bumpy papillary projections start appearing that are crusty to touch • Papillomas usually continue to grow at least 2–3 weeks post onset
Weeks 12–24	Papilloma growth/regression	• Subset of papillomas continue to persist and grow in size • Subset of papillomas continue to persist but start regressing • Subset of papillomas completely regress between 18 and 24 weeks PI